

Contribution to Proc. *NOON 2003: The 4th Workshop on Neutrino Oscillations and their Origin*, 10–14 February 2003, Kanazawa, Japan.

SUPERNOVA NEUTRINOS: FLAVOR-DEPENDENT FLUXES AND SPECTRA

GEORG G. RAFFELT AND MATHIAS TH. KEIL

*Max-Planck-Institut für Physik (Werner-Heisenberg-Institut)
Föhringer Ring 6, 80805 München, Germany*

ROBERT BURAS, HANS-THOMAS JANKA AND MARKUS RAMPP

*Max-Planck-Institut für Astrophysik
Karl-Schwarzschild-Str. 1, 85741 Garching, Germany*

Transporting ν_μ and ν_τ in a supernova (SN) core involves several processes that have been neglected in traditional simulations. Based on a Monte Carlo study we find that the flavor-dependent spectral differences are much smaller than is often stated in the literature. A full-scale SN simulation using a Boltzmann solver and including all relevant neutrino reactions confirms these results. The flavor-dependent flux differences are largest during the initial accretion phase.

1. Introduction

A supernova (SN) core is essentially a blackbody neutrino source, but in detail the fluxes and spectra depend on the flavor. Up to very small details ν_μ , ν_τ , $\bar{\nu}_\mu$ and $\bar{\nu}_\tau$ can be treated on an equal footing and will be collectively referred to as ν_μ . Numerical simulations usually find a hierarchy $\langle E_{\nu_e} \rangle < \langle E_{\bar{\nu}_e} \rangle < \langle E_{\nu_\mu} \rangle$ and approximately equal luminosities. The spectral differences offer an opportunity to observe flavor oscillations as the source fluxes will get partially interchanged. For example, it may be possible to distinguish a normal from an inverted neutrino mass hierarchy^{1,2,3,4}.

A full-scale numerical simulation by the Livermore group finds for the integrated signal $\langle E_{\nu_e} \rangle = 13$, $\langle E_{\bar{\nu}_e} \rangle = 16$ and $\langle E_{\nu_\mu} \rangle = 23$ MeV and almost perfect equipartition of the luminosities⁵, results that are representative for traditional numerical simulations. Sometimes extreme spectral hierarchies of up to $\langle E_{\bar{\nu}_e} \rangle : \langle E_{\nu_\mu} \rangle \approx 1 : 2$ have been stated, but searching the literature we find no support for such claims by credible simulations⁶.

Traditional numerical simulations treat the ν_μ and ν_τ transport somewhat schematically because their exact fluxes and spectra may not be im-

portant for the explosion mechanism. When a number of missing reactions are included one finds that $\langle E_{\bar{\nu}_e} \rangle$ and $\langle E_{\nu_\mu} \rangle$ are much more similar than had been thought. The remaining spectral and flux differences are probably large enough to observe oscillation effects in a high-statistics galactic SN signal, but the details are more subtle than had been assumed in the past.

2. Mu- and Tau-Neutrino Transport

The transport of ν_e and $\bar{\nu}_e$ is dominated by $\nu_e n \leftrightarrow pe^-$ and $\bar{\nu}_e p \leftrightarrow ne^+$, reactions that freeze out at the energy-dependent “neutrino sphere.” The flux and spectrum is essentially determined by the temperature and geometric size of this emission region. Moreover, the neutron density is larger than that of protons so that the $\bar{\nu}_e$ sphere is deeper than the ν_e sphere, explaining $\langle E_{\nu_e} \rangle < \langle E_{\bar{\nu}_e} \rangle$.

For ν_μ , in contrast, the flux and spectra formation is a three-step process. The main opacity source is neutral-current nucleon scattering $\nu_\mu N \rightarrow N\nu_\mu$. Deep in the star thermal equilibrium is maintained by nucleon bremsstrahlung $NN \leftrightarrow NN\nu_\mu\bar{\nu}_\mu$, pair annihilation $e^-e^+ \leftrightarrow \nu_\mu\bar{\nu}_\mu$ and $\nu_e\bar{\nu}_e \leftrightarrow \nu_\mu\bar{\nu}_\mu$, and scattering on electrons $\nu_\mu e^- \rightarrow e^-\nu_\mu$. The freeze-out sphere of the pair reactions defines the “number sphere,” that of the energy-changing reactions the “energy sphere,” and finally that of nucleon scattering the “transport sphere” beyond which neutrinos stream freely. Between the energy and transport spheres the neutrinos scatter without being absorbed or emitted and without much energy exchange, i.e. in this “scattering atmosphere” they propagate by diffusion.

One may think that the ν_μ spectrum is fixed by the medium temperature at the energy sphere so that $\langle E_{\bar{\nu}_e} \rangle < \langle E_{\nu_\mu} \rangle$ because the energy-sphere is deeper and hotter than the $\bar{\nu}_e$ sphere. However, the scattering atmosphere is more opaque to higher-energy neutrinos because the cross section scales as E_ν^2 , biasing the escaping flux to lower energies. For typical conditions $\langle E_{\nu_\mu} \rangle$ of the escaping flux is 50–60% of the value characteristic for the temperature at the energy sphere⁷. Therefore, the final $\langle E_{\bar{\nu}_e} \rangle : \langle E_{\nu_\mu} \rangle$ ratio is the result of two large counter-acting effects, the large temperature difference between the ν_μ energy sphere and the $\bar{\nu}_e$ sphere on the one hand, and the energy-dependent “filter effect” of the scattering atmosphere on the other.

Until recently all simulations simplified the treatment of ν_μ transport in that energy-exchange was not permitted in νN -scattering, e^-e^+ annihilation was the only pair process, and $\nu_\mu e$ -scattering was the only energy-exchange process. However, it has been recognized for some time

that nucleon recoils are important for energy exchange^{6,7,8}, that nucleon bremsstrahlung is an important pair process^{6,7,8,9,10,11,12}, and more recently that $\nu_e\bar{\nu}_e \rightarrow \nu_\mu\bar{\nu}_\mu$ is far more important than $e^-e^+ \rightarrow \nu_\mu\bar{\nu}_\mu$ as a $\nu_\mu\bar{\nu}_\mu$ source reaction^{6,13}.

We have performed a detailed assessment of the relevance of the new reactions on the basis of a Monte Carlo study⁶. To illustrate the results we use a hydrodynamically self-consistent accretion-phase model and show in Fig. 1 (left panel) the ν_μ flux spectrum when using the traditional input physics (bottom curve). Then we add nucleon bremsstrahlung that increases the flux without changing much the average energy. Next we switch on nucleon recoils that depletes the spectrum's high-energy tail without changing much the overall particle flux. Finally, switching on $\nu_e\bar{\nu}_e$ annihilation increases the flux without affecting the spectrum much. The compound effect of the new processes is not overly dramatic, but so large that all of them should be included in serious full-scale simulations.

In the right panel of Fig. 1 we compare for the same model the flux spectra of ν_e , $\bar{\nu}_e$ and ν_μ , the latter including all reactions. In this example $\langle E_{\bar{\nu}_e} \rangle$ almost exactly equals $\langle E_{\nu_\mu} \rangle$, but the fluxes differ by almost a factor of 2. This is reverse to the usual assumption of a pronounced hierarchy of average energies and nearly exact equipartition of the luminosities.

We have studied a variety of stellar background models, some of them self-consistent hydrostatic models, others power-law profiles of density and temperature. For realistic cases we never find extreme spectral hierarchies,

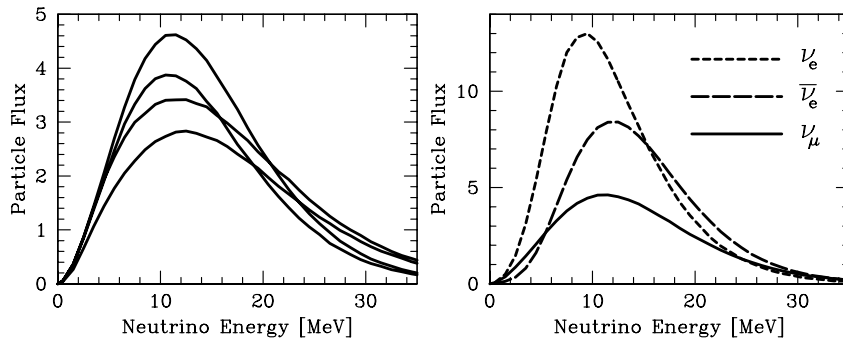


Figure 1. Neutrino fluxes for an accretion-phase model. *Left panel*, curves from bottom to top: Flux of ν_μ with traditional neutrino interaction channels, then adding nucleon bremsstrahlung, next adding nucleon recoils, and finally adding $\nu_e\bar{\nu}_e$ annihilation. *Right panel*: Fluxes for all flavors; the ν_μ curve includes all reaction channels.

the differences between $\langle E_{\bar{\nu}_e} \rangle$ and $\langle E_{\nu_\mu} \rangle$ typically being 0–20%. On the other hand, the fluxes can be rather different, especially during the accretion phase when the atmosphere is quite extended. The different neutrino spheres have then rather different geometric extensions, explaining large flux differences. Later during the Kelvin-Helmholtz cooling phase the star is very compact so that any geometry effect of the radiating surfaces is small. Moreover, the relevant regions are then neutron rich so that the transport physics of $\bar{\nu}_e$ and ν_μ will become similar. Therefore, during the late phases one expects very similar $\bar{\nu}_e$ and ν_μ fluxes, while, of course, the ν_e flux and spectrum remain unaffected by our arguments.

3. Spectral Characteristics

To characterize the neutrino fluxes one naturally uses some global parameters such as the particle flux, the luminosity (energy flux), and the average energy $\langle E \rangle$. In order to characterize the spectral shape in greater detail one may also invoke higher energy moments $\langle E^n \rangle$. One measure frequently given from numerical simulations is $E_{\text{rms}} = \sqrt{\langle E^3 \rangle / \langle E \rangle}$ because of its relevance for calculating average neutrino-nucleon interaction rates.

Sometimes a global analytic fit to the spectra is also useful. Frequently one approximates the flux spectra by a nominal Fermi-Dirac function

$$f(E) \propto \frac{E^2}{1 + \exp(-\eta + E/T)} \quad (1)$$

with a temperature T and a degeneracy parameter η . This approximation allows one to fit the overall luminosity and two energy moments, typically chosen to be $\langle E \rangle$ and $\langle E^2 \rangle$. However, the Fermi-Dirac fit is not more natural than other possibilities; certainly the low- and high-energy tails of the spectra are not especially well represented by this fit.

We find that the Monte Carlo spectra are approximated over a broader range of energies by a simpler functional form that we call “alpha fit,”

$$f(E) \propto E^\alpha \exp [-(\alpha + 1) E / \bar{E}] . \quad (2)$$

For any value of α we have $\langle E \rangle = \bar{E}$, a Maxwell-Boltzmann spectrum corresponds to $\alpha = 2$. The numerical spectra show values of $\alpha = 2.5$ –5, i.e. they are “pinched.”

4. A Full-Scale Simulation

In the Garching SN code¹⁴ we have now implemented all relevant neutrino interaction rates, including nucleon bremsstrahlung, neutrino pair processes, weak magnetism, and nucleon recoils. Our treatment of neutrino-nucleon interactions includes nuclear correlation effects. The transport part of this code is based on a Boltzmann solver. The neutrino-radiation hydrodynamics program enables us to perform spherically symmetric as well as multi-dimensional simulations, thus allowing us to take into account the effects of convection.

To explore the time-dependent properties and long-time evolution of the neutrino signal, we currently continue a state-of-the-art hydrodynamic calculation of a SN into the Kelvin-Helmholtz neutrino cooling phase of the forming neutron star. The progenitor model is a $15 M_{\odot}$ star with a $1.28 M_{\odot}$ iron core (Model s15s7b2 from S. Woosley; personal communication). The period from shock formation to 480 ms after bounce was evolved in two dimensions. The subsequent evolution of the model is simulated in spherical symmetry. At 150 ms the explosion sets in, driven by neutrino energy deposition and aided by very strong convective activity in the neutrino-heating region behind the shock (Fig. 2). Note that a small modification of the Boltzmann transport was necessary to allow the explosion to happen¹⁵. Unmanipulated full-scale models with an accurate treatment of the micro-

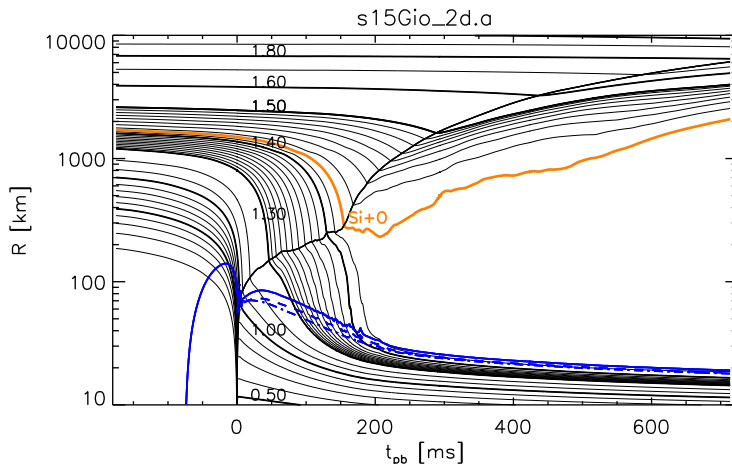


Figure 2. Trajectories of the mass shells in the core of an exploding $15 M_{\odot}$ star. The explosion occurs about 150 ms after shock formation, developing a bifurcation (“bubble”) between the mass that follows the outgoing shock and the mass that settles on the nascent neutron star. Also indicated are the positions of the neutrino spheres of ν_e , $\bar{\nu}_e$ and ν_{τ} .

physics currently do not obtain explosions¹⁶. Details of this run will be documented elsewhere; at the time of this writing the CPU expensive calculation is still on the computer. Here we show in Fig. 3 a preview of the main characteristics of the neutrino signal up to 750 ms post bounce.

The neutrino signal agrees with what is expected for the standard delayed-explosion scenario. In particular, it clearly shows the prompt ν_e burst and a broad shoulder in all fluxes during the accretion phase that ends at 200 ms when the explosion has taken off. The average neutrino energies follow the usual hierarchy and they increase with time due to the contraction of the star. We also show the alpha parameter from a global fit according to Eq. (2). During the accretion phase the ν_μ flux is least pinched, at late times the α values of all flavors converge near 2.5.

These results agree with and nicely illustrate our previous Monte Carlo findings in that the spectral hierarchy between $\bar{\nu}_e$ and ν_μ is rather mild and

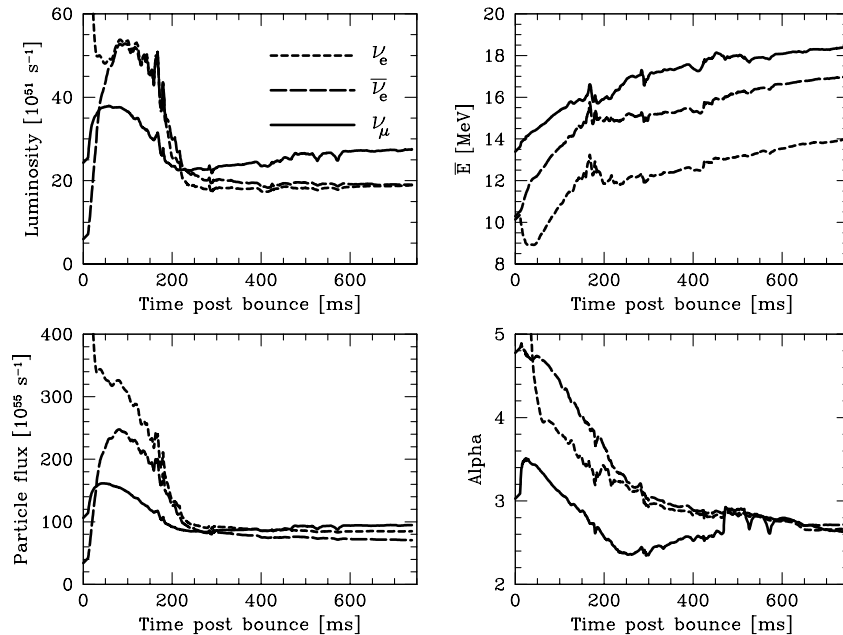


Figure 3. Neutrino fluxes and spectral properties for the full-scale simulation described in the text. The hydrodynamic bounce and shock formation occur at $t = 0$ (cf. Fig. 2). The right upper plot gives the spectral fit parameter \bar{E} , the right lower one α . Note that the discontinuity in the latter at $t \approx 480$ ms is caused by mapping the model from two dimensions to one.

in that the average energies converge at late times. Conversely, the particle fluxes differ by almost a factor of 2 during the accretion phase, but cross over shortly after the explosion. At 750 ms the differences between the fluxes continue to increase, an asymptotic value has not yet been reached.

5. Conclusions

Traditional numerical SN simulations had two weaknesses regarding the flavor-dependent neutrino fluxes and spectra. First, the interaction between $\nu_{\mu,\tau}$ and $\bar{\nu}_{\mu,\tau}$ and the stellar medium was schematic, neglecting a number of important processes. Second, a Boltzmann solver for neutrino transport could not be coupled self-consistently with the hydrodynamic evolution.

We have performed a systematic Monte Carlo study on various stellar background models and the first SN simulation that includes all relevant interaction rates and a Boltzmann solver. While the usual relationship between the ν_e and $\bar{\nu}_e$ fluxes and spectra remains essentially unchanged, the ν_μ spectrum is much more similar to that of $\bar{\nu}_e$, especially during the Kelvin-Helmholtz cooling phase. Differences of the average energies are in the range 0–20%, with 10% being a typical number. During the accretion phase the ν_μ particle flux is smaller than that of $\bar{\nu}_e$ by up to a factor of 2, but later the particle fluxes cross over.

Our findings imply that observing neutrino oscillation effects in a SN signal is a more subtle problem than had been thought previously, but by no means impossible. However, when exploring the physics potential of a future galactic SN one should not rely on the notion of an exact flavor equipartition of the luminosities or the extreme spectral differences that have sometimes been stated in the literature.

Acknowledgments

This work was supported, in part, by the Deutsche Forschungsgemeinschaft under grant No. SFB-375 and by the European Science Foundation (ESF) under the Network Grant No. 86 Neutrino Astrophysics.

References

1. A. S. Dighe and A. Y. Smirnov, “Identifying the neutrino mass spectrum from the neutrino burst from a supernova,” *Phys. Rev. D* **62**, 033007 (2000) [hep-ph/9907423].
2. C. Lunardini and A. Y. Smirnov, “Probing the neutrino mass hierarchy and the 13-mixing with supernovae,” hep-ph/0302033.

3. K. Takahashi and K. Sato, “Effects of neutrino oscillation on supernova neutrino: Inverted mass hierarchy,” hep-ph/0205070.
4. K. Takahashi and K. Sato, “Earth effects on supernova neutrinos and their implications for neutrino parameters,” *Phys. Rev. D* **66**, 033006 (2002) [hep-ph/0110105].
5. T. Totani, K. Sato, H. E. Dalhed and J. R. Wilson, “Future detection of supernova neutrino burst and explosion mechanism,” *Astrophys. J.* **496**, 216 (1998) [astro-ph/9710203].
6. M. T. Keil, G. G. Raffelt and H.-T. Janka, “Monte Carlo study of supernova neutrino spectra formation,” astro-ph/0208035.
7. G. G. Raffelt, “Mu- and tau-neutrino spectra formation in supernovae,” *Astrophys. J.* **561**, 890 (2001) [astro-ph/0105250].
8. H.-T. Janka, W. Keil, G. Raffelt and D. Seckel, “Nucleon spin fluctuations and the supernova emission of neutrinos and axions,” *Phys. Rev. Lett.* **76**, 2621 (1996) [astro-ph/9507023].
9. H. Suzuki, “Neutrino emission from proton-neutron star with modified Urca and nucleon bremsstrahlung processes,” *Num. Astrophys. Japan* **2**, 267 (1991).
10. H. Suzuki, “Supernova neutrinos—Multigroup simulations of neutrinos from proton-neutron star,” in: Proc. International Symposium on Neutrino Astrophysics: Frontiers of Neutrino Astrophysics, 19–22 Oct. 1992, Takayama, Japan, edited by Y. Suzuki and K. Nakamura (Universal Academy Press, Tokyo, 1993).
11. S. Hannestad and G. Raffelt, “Supernova neutrino opacity from nucleon nucleon bremsstrahlung and related processes,” *Astrophys. J.* **507**, 339 (1998) [astro-ph/9711132].
12. T. A. Thompson, A. Burrows and J. E. Horvath, “Mu and tau neutrino thermalization and production in supernovae: Processes and timescales,” *Phys. Rev. C* **62**, 035802 (2000) [astro-ph/0003054].
13. R. Buras, H.-T. Janka, M. T. Keil, G. G. Raffelt and M. Rampp, “Electron-neutrino pair annihilation: A new source for muon and tau neutrinos in supernovae,” *Astrophys. J.*, in press (2003) [astro-ph/0205006].
14. M. Rampp and H.-T. Janka, “Radiation hydrodynamics with neutrinos: Variable Eddington factor method for core-collapse supernova simulations”, *Astron. Astrophys.* **396**, 361 (2002) [astro-ph/0203101].
15. H.-T. Janka, R. Buras, K. Kifonidis, T. Plewa and M. Rampp, “Explosion Mechanisms of Massive Stars”, in: *Core Collapse of Massive Stars*, edited by C.L. Fryer (Kluwer Academic Publ., Dordrecht, 2003) [astro-ph/0212314].
16. R. Buras, M. Rampp, H.-T. Janka and K. Kifonidis, “Improved models of stellar core collapse and still no explosions: What is missing?”, *Physical Review Letters*, submitted (2003) [astro-ph/0303171].